Influence of fabric structure on electrical resistance of graphene-coated textiles

RUIZ-CALLEJA Tamara[1], BONET-ARACIL Marilés[2], GISBERT-PAYÁ Jaime[2], BOU-BELDA Eva[2], MONTAVA Ignacio[2], CALDERÓN-VILLAJOS Rocío[1]

[1]Universidad Rey Juan Carlos, Calle Tulipán, 28933 Móstoles, Spain

[2]Universitat Politècnica de València, Textile and Paper Department, Plaza Ferrándiz y Carbonell s/n, 03801, Alcoy, Spain.

Corresponding author: Ruiz-Calleja, T. Calle Tulipán, 28933 Móstoles, Spain. E-mail: tamara.ruiz@urjc.es

Abstract Coating is a widespread technique in the textile industry for different purposes, mainly in coloring and functional finishes. Graphene is usually applied to fabrics using coating techniques to provide such fabrics with properties like thermal or electrical conductivity. All woven fabrics have peaks and valleys in their structure, generated by the warp and weft threads interlacing. When spreading the graphene coating, the paste is placed in the fabric's interstices, and the connection between conductive particles is only produced when the height of the coating is sufficient to connect the different areas where it is deposited. This article analyzes three types of satin weave with three interlacing coefficients (0.4, 0.25, 0.17) and two sets of weft yarns each (20 and 71.43 tex). For a blade gap of 1.5 mm, the electrical resistance of samples with weft yarn count of 20 tex and interlacing coefficient of 0.4 is 534.33 Ω, while for IC = 0.25 electrical resistance is 36.8% higher and for IC = 0.17 this parameter increases 249.3%. For samples with weft yarn count of 71.43, the sample with IC = 0.40 exhibits an electrical resistance of 1053 Ω, for IC = 0.25 this value rises to 33.9% and for IC = 0.17 the electrical resistance value increases a total of 78.9%. This finding can be of interest for coatings where continuity is crucial, and for the application of substances that need to be protected from external factors, for which fabrics with deep interstices can be designed to house said products.

Key words: graphene, coating, textile, conductive, weave pattern, interlacing coefficient, satin weave, electrical resistance

1. Introduction

Mechanical,[1, 2] electrical,[3-5] and thermal[6, 7] properties of graphene make this material an element with enormous potential for various applications, such as manufacturing devices for energy storage and generation,[8, 9] sensors,[10] or drug release mechanisms.[11-13] With a two-dimensional structure, graphene is composed of carbon

atoms arranged in a flat hexagonal mesh [14] and has a specific surface weight of 7.602 × 10^{-4} g m^{-2}.[15] This material, discovered in 2004,[5] has also found its place in the field of textiles, especially in the area of intelligent and functional textiles,[16-18] where it is usually applied as a fluid coating to fabrics and yarns[19-22] and also manufactured as nanofibers[23, 24] or woven meshes.[25, 26]

The fluid coating procedure can be carried out using different techniques, including knife-coating, roll-coating, impregnation, and spray-coating.[27] For all these techniques, a vast bibliography evaluates how the different aspects of the coating process influence the result, such as the angle of inclination when there is a blade, the variation of the coating thickness, or the speed of the operation, among many other factors for textile finishing.[27-31]

The weave structure or pattern of a fabric[32] and the interlacing coefficient (IC)[33] have been analyzed to determine specific characteristics of the fabrics, mainly their mechanical properties. Farboodmanesh et al.[34] provide a comprehensive research on how the structure of fabrics can interfere with coatings and the effect a textile structure has on coating penetration and thickness, concluding that a looser satin weave would generate better results for greater coating penetration. Additionally, other authors[35] analyze the contribution of cloth geometry to the abrasion-resistance of textile fabrics. Calvimontes et al.[36] study how the topographical characteristics affects the wettability of the fabrics, finding out the water contact angle increases when the surface roughness of the fabric does. The relationship between electromagnetic shielding effectiveness (EMSE) with the weave pattern has been analyzed by Özdemir et al.,[37] detecting that the average float length, the weave interlacing coefficient, and the arrangement of yarn floats have significant effects on the EMSE performance of the fabrics examined. Furthermore, Berruezo et al.[38] have evaluated the generation of microplastics when laundering different weave patterns and determined that the quantity of fibers released into the wastewater is inversely proportional to the IC. However, the influence of the weave pattern of a fabric or its IC on the final performance of coatings made with conductive elements such as graphene has not been evaluated so far.

In this study, the behavior, in terms of electrical resistance, of three types of satin weave with two different sets of weft yarns, knife-coated with graphene is analyzed, to determine whether there is a relationship between the fabric structure and the performance of the conductive coating. Likewise, three different graphene concentrations in the coating paste and several gaps of the blade are examined. After the tests carried out, it is found the weave pattern and IC significantly influence the resistance results obtained. Therefore, this finding opens an exciting line of research toward developing functional and intelligent fabrics, where it is vital to identify the most suitable weave pattern to achieve the best results in each case. The novelty of

this work resides in the study carried out on how the structure of the fabric can dictate where the coating is deposited and, therefore, influence the electrical conductivity results. This relationship has not been previously studied in the existing literature and its implications are of interest for textile fields where a product is applied to a fabric through coating techniques, including conductive particles, but also extendable to a wide range of substances like microcapsules or active ingredients.

2. Experimental

2.1. Materials

For this research, the fabric samples used are listed in Table 1, all of them 100% polyester with a satin weave pattern. Warp density is 60 threads/cm. Warp yarn is a tangled multifilament PES 167 dtex/48 filaments. Two different sets of weft yarns are used, 20 tex and 71.43 tex, both single-ply PES yarns. Each weave pattern is designed to reach maximum weft density. The samples are produced using a Smit GS 900 weaving machine of 190 cm width, with a Stäubli DX-100 electronic Jacquard machine and EAT DesignScope software.

Reference	Rapport	Course	Weft yarn count (tex)	Weft density (threads/cm)	Weight (g/m^2)	IC	Thickness (mm)
P5-20	3e2	5 x 5	20	33	198	0.40	0.49
P8-20	5e3	8 x 8	20	37	200	0.25	0.59
P12-20	7e5	12 x 12	20	43	213	0.17	0.61
P5-71	3e2	5 x 5	71.43	20	290	0.40	0.65
P8-71	5e3	8 x 8	71.43	23	307	0.25	0.78
P12-71	7e5	12 x 12	71.43	26	331	0.17	0.80

Table 1. Fabric samples characteristics.

Figure 1 depicts the samples' rapport, and Figure 2 displays a three-dimensional representation of the fabrics.

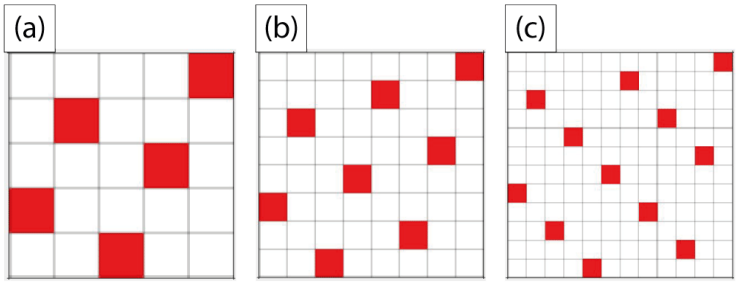

Figure 1. Weave diagram of (a) Satin 3e2; (b) Satin 5e3; (c) Satin 7e5.

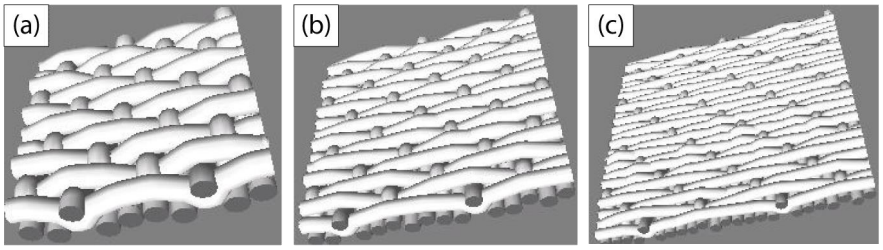

Figure 2. 3D representation of (a) Satin 3e2; (b) Satin 5e3; (c) Satin 7e5.

Figures 1.a and 2.a belong to the 3e2 satin, the smallest course possible for said weave pattern, where it can be observed that the number of interlacing points amounts to 10. In the images corresponding to 5e3 and 7e5 satins, the course of the weave pattern increases, and so does the number of interlacing points, however the IC decreases.

Graphene, with an average size of 30 x 40 µm and 10 nm of thickness, synthesized by a modified Hummers method using flake graphite powders as the starting material, is supplied by Innovatec SC, S.L.

Coating paste is obtained using the following products:

- Acrylic binder STK-100 supplied by Color-Center S.A.,
- Thickener Lutexal CSN and fixing agent Luprintol SE, supplied by Archroma and
- Ammonia 28% supplied by Prolabo.

2.2. Fabric coating procedure

The quantity of each product used for the base coating paste, according to binder's supplier instructions, are described in Table 2:

Product	Quantity (g/kg)
Thickener	20
Binder	10
Fixing agent	10
Ammonia	10

Table 2. Base coating paste composition.

For comparison, different concentrations of graphene have been used for the conductive coating: 12, 18, and 24 g/kg, and each sample reference is followed by G12, G18, or G24 according to the amount of graphene used in the coating. The coating paste is obtained through mechanical stirring at 2000 rpm for 300 seconds.

Higher concentrations of graphene are not tested due to the rheological properties of the coating paste. Rheological properties of the graphene paste are measured with a rotational viscometer (ViscoElite-R, Fungilab, Spain). The spindle is selected according to the values recommended by the provider, it is immersed in the paste with 45º angle and gradually placed vertically till it is connected to the viscosimeter.

Afterwards the viscosimeter position is adjusted so as to cover with the paste the recommended length of the spindle.

Coating paste deposition onto fabric is performed through knife-coating using a metallic surface and an adjustable blade, as seen in Figure 3, set at different heights, from 0.5 to 1.5 mm at intervals of 0.125 mm.

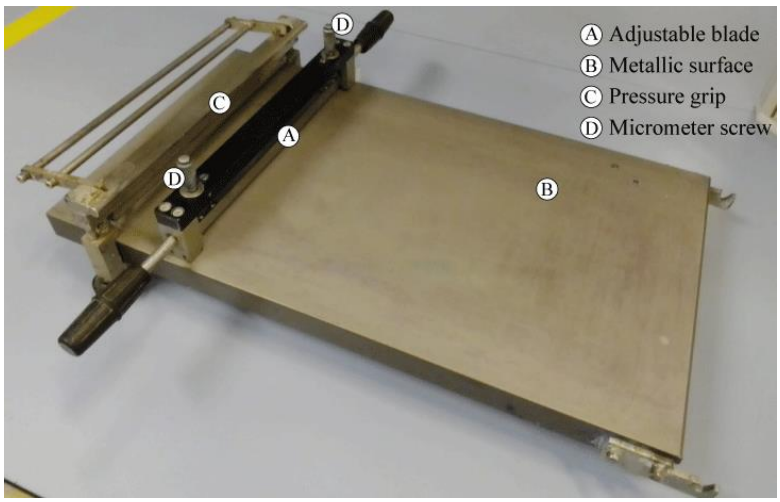

Figure 3. Coating equipment.

Fabric samples with a size of 15 x 50 cm are fixed to the metal frame with a pressure grip. The coating paste is poured onto the fabric, and the blade is positioned at an angle of 90º and a gap of 1.5 mm between the blade and the surface. Every 5 cm the gap is reduced by 0.125 mm using the micrometer screw. The excess of coating paste is then removed, and the samples are oven-dried at 60 °C for 1 hour. Figure 4 shows a schematic representation of the coating process described above.

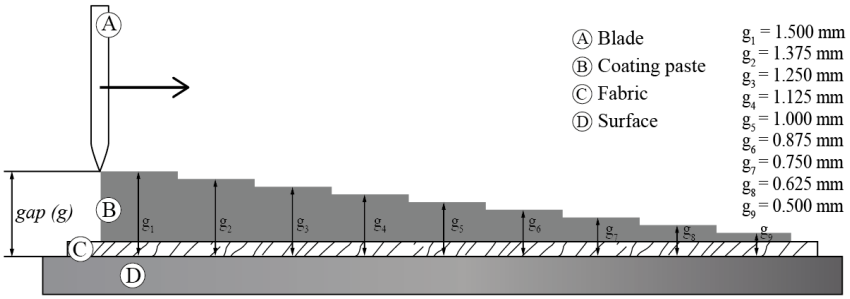

Figure 4. Schematic representation of the coating process.

2.3. Sample characterization

The observation of the samples is carried out using a Field Emission Scanning Electron Microscope (FESEM) (ULTRA 55, ZEISS). To analyze samples by SEM, each of them is placed on a surface and covered with a thin layer of gold and palladium to transform them into conductive by using a Sputter Coater. The samples are analyzed with the appropriate magnification and with an acceleration voltage of 2 kV in SEM.

Topographic images of the fabric are obtained using a 3D optical profiler from Zeta Instruments (Zeta-20 model) and subsequently processed with Mountain Map Premium 7.1 software.

2.4. Electrical resistance evaluation

The electrical resistance of graphene-coated fabric is evaluated using a Fluke 115 digital multimeter. All the samples are cut down to 1 cm^2 and resistance is tested out placing multimeter leads in opposite corners. Three samples cut from different areas of the coated fabric have been analyzed and the average value is presented in this work.

2.5. Statistical analysis

An analysis of variance (ANOVA) test is performed for each graphene concentration, comparing the interaction between gaps (where electrical resistance is lower than infinite) and the different weave patterns, to assess their significance in the electrical resistance values obtained.

3. Results and discussion

3.1. Electrical resistance

Figures 5, 6, and 7 represent mean values of electrical resistance data retrieved from all samples, coated with three concentrations of graphene and gaps from 0.5 to 1.5 mm, as stated in section 2.2.

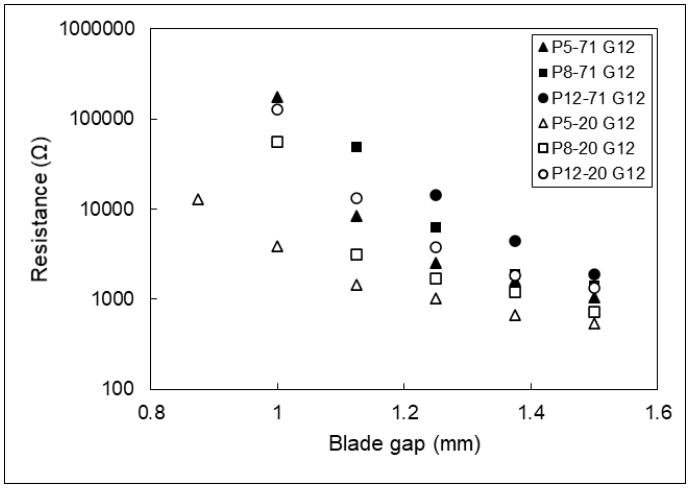

Figure 5. Electrical resistance of samples coated with G12.

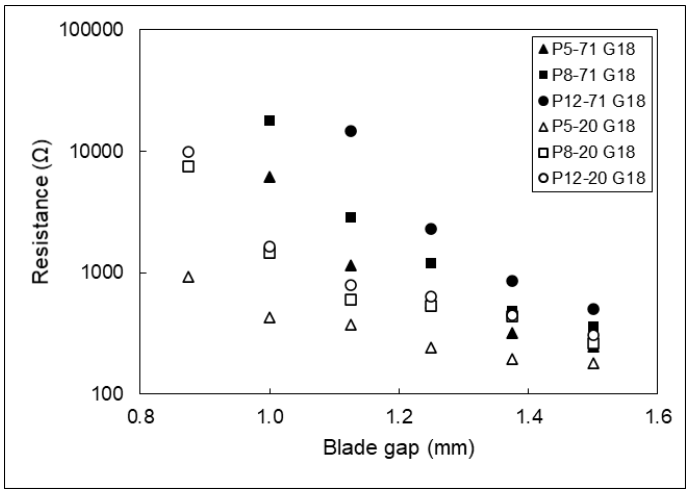

Figure 6. Electrical resistance of samples coated with G18.

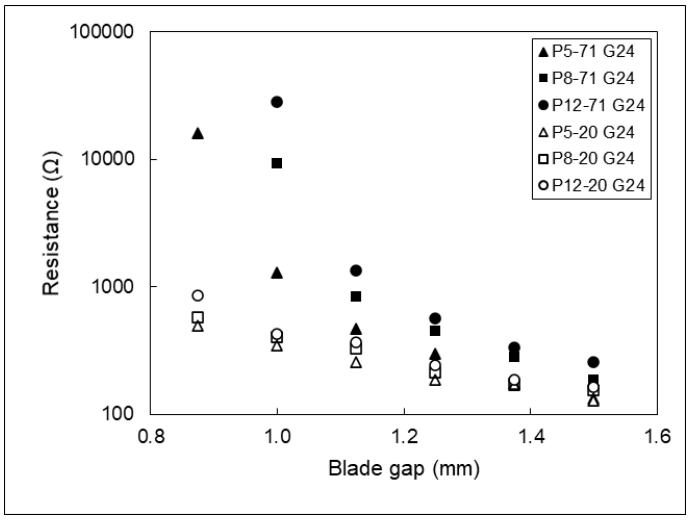

Figure 7. Electrical resistance of samples coated with G24.

When the amount of graphene within the coating paste increases, the conductivity of said coating improves as expected. For sample P5-20-G24$_{1.000}$, electrical resistance is 349.67 Ω, for P5-20-G18$_{1.000}$ it is 433 Ω, while for P5-20-G12$_{1.000}$ this value is 3853.33 Ω, noting that the increase in resistance is not linear but exponential as seen in Figure 8. This phenomenon is attributed to the fact that more graphene in the coating paste means a greater presence of conductive particles throughout the coating volume, which form a higher number of connection points through which electricity is transported. However, the fact that these particles are two-dimensional significantly reduces the chances of establishing connection points when the quantity of graphene incorporated into the coating paste is lowered. This difference in the resistance value is much more noticeable in smaller gaps because the coating volume is reduced and, consequently, the amount of graphene incorporated on the fabric.

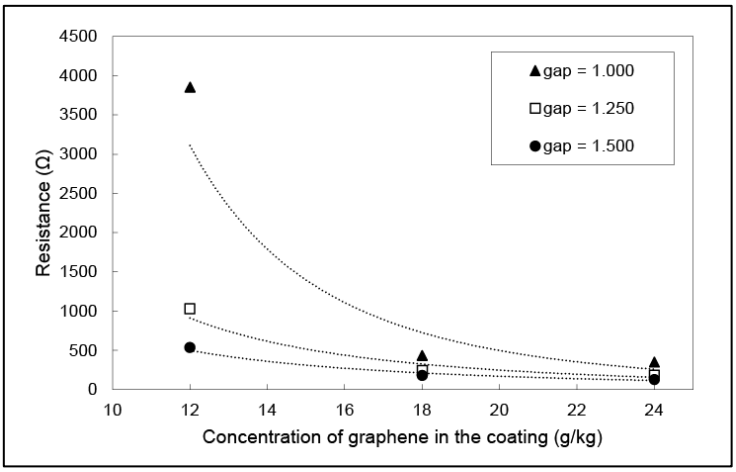

Figure 8. Correlation between concentration of graphene and resistance of P5-20 for gaps 1.500, 1.250, and 1.000 mm.

For higher blade gaps, the variation in electrical resistance becomes less noticeable since the maximum conductivity that a specific concentration of graphene can provide is reached, and it will not improve significantly despite depositing a larger quantity of coating paste. For example, P5-20-G24$_{1.500}$ has a resistance value of 126.93 Ω, while P5-20-G24$_{1.375}$ resistance is 169.40 Ω. In previous internal studies, it has been identified that for gaps greater than 1.5 mm, the changes in the resistance values are minimal. The percolation threshold for a gap of 1.5 mm is achieved by incorporating between 0.6 and 0.8 graphene wt% to the coating paste.

However, the most significant and novel result is obtained when comparing the variation in resistance between the different weave patterns and their IC. It is observed that the change in the structure of the weave pattern also generates changes in conductivity. As seen in Figure 9, the samples with an IC equal to 0.4 exhibit the lowest resistance value in all cases, while, when increasing the IC, the resistance values also increase. This phenomenon occurs because, when modifying the weave pattern, there is also a modification in the surfaces of the fabrics, generating areas with greater height (peaks) or depth (valleys), depending on each case, and this affects the deposition of the coating paste on the fabric. For weave patterns with higher IC, the number of interlacing points is greater and there are less floatations, which provides a more uniform surface than in weave patterns with lower IC. When there is less difference in height between peaks and valleys, the coating has better continuity than in structures where this height is greater and a larger amount of coating is necessary to bridge the distance between peak and valley to maintain conductivity.

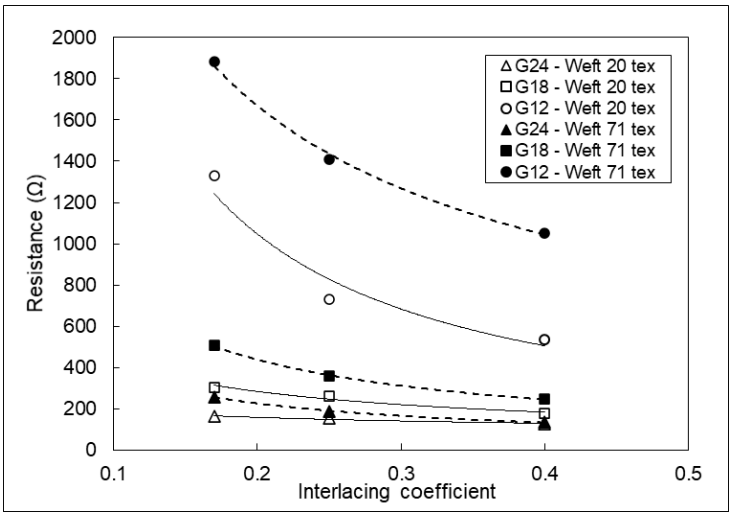

Figure 9. Resistance of all samples at gap 1.500 mm.

Furthermore, when the weft yarn count increases the surface of the fabric becomes more irregular, resulting in broader height differences between the thicker weft yarns and the thinner warp yarns, which has a moderate impact on the coating resistance, especially in weave patterns 5e3 and 7e5.

It is also observed that there are higher standard deviations with smaller gaps, but this trend is not constant in all cases. This anomaly is attributed to where measurements are taken, which may correspond to a peak or a valley area, and produce that measurement variation. Additionally, it is found that the minimum blade gap to produce conductivity differs depending on the weave pattern used in each case, therefore it should be considered when manufacturing fabrics with conductive coatings.

Analyzing the electrical resistance values obtained for gaps 1.500, 1.375, and 1.250 mm, a synthetic index is proposed to relate the resistance value with the IC, blade gap, weft yarn count, and graphene concentration of each sample.

$$R = \frac{k_1}{IC^{k_2}} \qquad \text{(Equation 1)}$$

Equation 1 exhibits said correlation where k_1 and k_2 are parameters specific to each concentration, weft yarn count, and blade gap, listed in the following table:

gap (mm)	*1.5*		*1.375*		*1.250*	
	k_1	k_2	k_1	k_2	k_1	k_2
G12-Weft 20 tex	192.420	1.053	226.260	1.192	241.490	1.512
G18-Weft 20 tex	102.960	0.630	85.917	1.000	92.141	1.143
G24-Weft 20 tex	98.930	0.290	151.780	0.109	139.170	0.311
G12-Weft 71 tex	561.300	0.678	487.370	1.168	384.100	2.041
G18-Weft 71 tex	112.840	0.843	105.720	1.158	128.740	1.619
G24-Weft 71 tex	65.727	0.767	88.650	0.779	150.690	0.762

Table 3. Parameters k_1 and k_2 for Equation 1.

Tables 4 to 6 include the results for ANOVA tests to evaluate the significant factors affecting the electrical resistance for each concentration. Fabric structure and

gap are found to have a significant effect within the electrical resistance results obtained, with p values lower than 0.05.

Source of Variation	*SS*	*df*	*MS*	*F*	*P-value*	*F crit*
Gap	147114574.3	2	73557287.17	1444.293125	4.21003×10^{-35}	3.259446306
Fabric	229251282.6	5	45850256.52	900.2671633	9.75061×10^{-37}	2.477168673
Interaction	180381340.6	10	18038134.06	354.17773	7.87012×10^{-33}	2.10605391
Within	1833466	36	50929.61111			
Total	558580663.5	53				

Table 4. ANOVA results for concentration G12.

Source of Variation	*SS*	*df*	*MS*	*F*	*P-value*	*F crit*
Gap	113122172.9	3	37707390.95	1533.4409	1.20717×10^{-47}	2.798060635
Fabric	163828231.5	5	32765646.3	1332.4757	3.04141×10^{-50}	2.408514119
Interaction	313002693.9	15	20866846.26	848.5889555	7.73007×10^{-53}	1.880174584
Within	1180322.48	48	24590.05167			
Total	591133420.7	71				

Table 5. ANOVA results for concentration G18.

Source of Variation	*SS*	*df*	*MS*	*F*	*P-value*	*F crit*
Gap	577061860.2	4	144265465.1	3509.193099	2.29359×10^{-70}	2.525215102
Fabric	415127986.2	5	83025597.24	2019.560626	1.80058×10^{-65}	2.368270236
Interaction	1435738123	20	71786906.14	1746.184477	2.22966×10^{-75}	1.747984133
Within	2466643.373	60	41110.72289			
Total	2430394613	89				

Table 6. ANOVA results for concentration G24.

3.2. Topographic images

Figure 10 shows the topographic analysis of samples P5-20, P8-20, and P12-20. Each point of the fabric surface has a specific color depending on its height, according to the color scale on the right of the images.

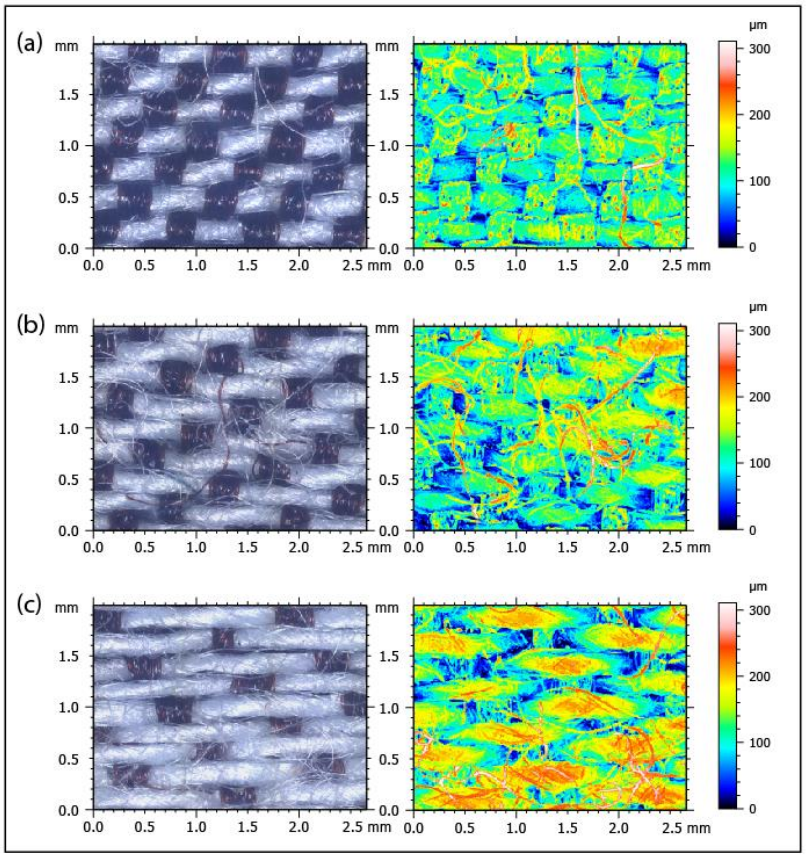

Figure 10. Topographic images of samples (a) P5-20, (b) P8-20, and (c) P12-20.

To compare the three topographic images, a value of 150 µm is established as height reference for being the mean value of the scale. Using image analysis software, the sample area below and above the height reference value are calculated. Figure 10.a demonstrates that the difference in height between the peaks and valleys in sample P5-20 is minimal, with 74.79% of its surface below 150 µm and 25.21% above said value, being 210 µm the maximum height reached. With such a low difference between peaks and valleys within the structure, the conductive coating has adequate continuity. Even in smaller coating gaps, the height that needs to be bridged is less than in the rest of the samples, which is reflected in the resistance values provided in Figures 5 to 7.

Regarding Figure 10.b, obtained from sample P8-20, there is a more significant difference between the areas with less depth and greater height, with 66.10% of the studied area below 150 µm and 33.90% above 150 µm. This height difference produces valleys in which the coating accumulates, which are isolated from other areas because of the peaks. No connection occurs between conductive particles when the coating thickness is not enough to exceed the peaks' height. This phenomenon directly affects the coating's conductivity, as seen in Figures 5 to 7, where there is a significant variation between electrical resistance exhibited by samples P5-20 and P8-20.

In Figure 10.c, which belongs to sample P12-20, the trend described in the previous samples is found again, where the contrast between deeper and higher areas increases, with 53.61% of the topographic image below 150 μm and 46.39% above that value. Furthermore, weft flotations are particularly long in this weave pattern, causing higher peaks in the weft direction than the previous samples. When applying the conductive coating, it tends to deposit in the interstices formed by the fabric, hence for the same gap, the level of resistance in this weave pattern is higher than for the previous structures studied, as reflected in Figures 5 to 7.

3.3. Coating properties

Figure 11 summarizes viscosity results for graphene concentrations from 0 to 36 g/kg, where three measurements are obtained for each concentration, and the mean value is displayed. The low density of graphene[15] implies that, even in small grammages, is incorporation in the coating paste means adding a considerable volume of dry and hydrophobic product, which substantially increases the viscosity of the solution and hinders its homogeneous spread.

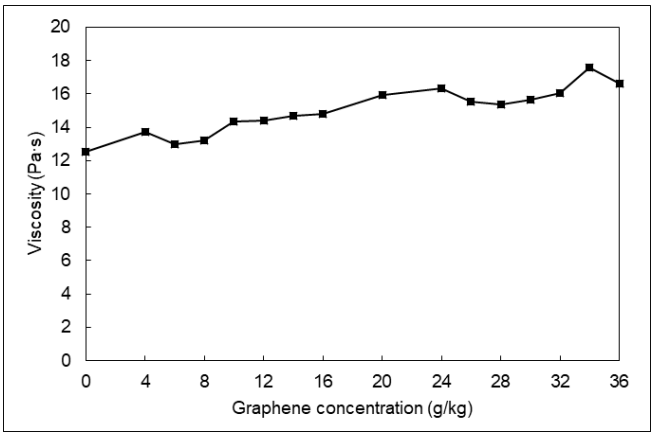

Figure 11. Viscosity of the coating paste with different concentrations of graphene.

The amount of coating paste deposited on each sample is driven by the gap at which the blade is set and the structure of the fabric. Figure 12 includes the weights of the dried coating paste for each gap and weave pattern.

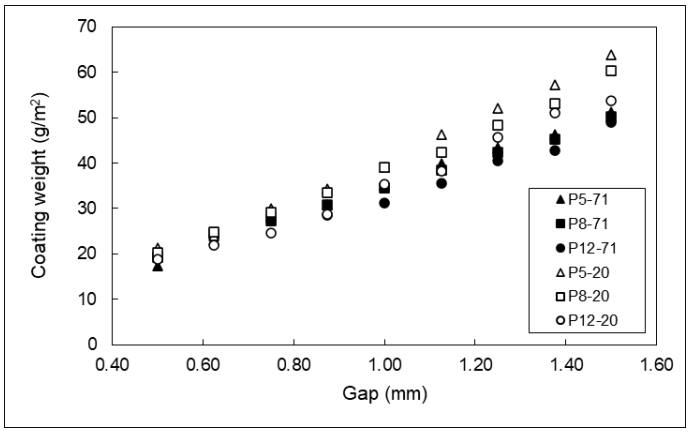

Figure 12. Coating weight for each gap and weave pattern.

For a gap of 1.5 mm, around 1500 g/m^2 of coating solution are added which, after drying, lose about 95% of water weight. Three concentrations of graphene are tested in grams per kilogram of coating paste (12, 18, and 24 g/kg). For 1500 g/m^2 of paste, 18, 27, and 36 g of graphene are added to the fabric. To analyze electrical resistance, 1 cm^2 of fabric is evaluated, that means in each sample there are 1.8, 2.7, and 3.6 mg of graphene, respectively.

Using topographic image analysis, the peak and hole volumes of samples P5-20, P8-20, and P12-20 are studied in an area of 1 mm^2, to understand the volume that can be filled by the coating solution and its relationship with the IC. Table 7 gathers the information retrieved from the topographical analysis:

Reference	Hole volume (mm³)	Peak volume (mm³)	Interlacing coefficient
P5-20	0.018351236	0.020780237	0.40
P8-20	0.020138139	0.02137604	0.25
P12-20	0.018726038	0.027285592	0.17

Table 7. Hole and peak volume analysis of samples P5-20, P8-20, and P12-20.

When the structure of the weave pattern does not exhibit a significant difference between peaks and valleys, as seen in Figure 10.a for P5-20, the coating paste is gently spread all over the surface. However, if there is a prominent presence of peaks in the weave pattern, as in Figures 10.b and 10.c, said peaks have an impact on the amount of coating deposited: as they fill a certain volume, the paste will not be able to fill the space already occupied by the peaks and will be deposited in the interstices of the fabric. Regarding the hole volume calculated in Table 7, there is practically no difference between the three samples studied. However, the difference is quite significant for the peak volume, where this value increases as the IC decreases. For the same blade gap, a weave pattern with a higher IC will be coated with more paste than a fabric with lower IC, because the peaks occupy a certain volume instead of the coating solution.

3.4. SEM images

Images of the uncoated fabrics are seen in Figure 13. It is worth highlighting each of the samples has a specific set of interstices and peaks depending on its weave pattern, which dictate the way the coating solution is deposited and to what degree it affects the electrical resistance values obtained.

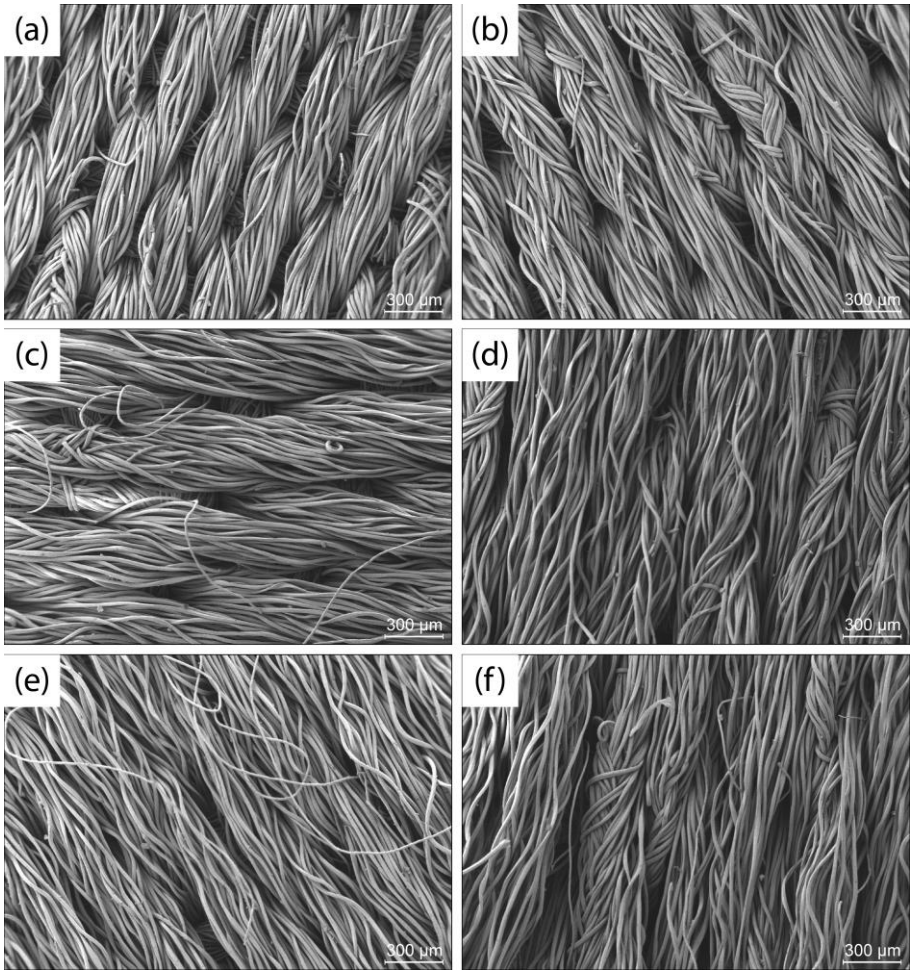

Figure 13. SEM images of samples (a) P5-20; (b) P5-71; (c) P8-20; (d) P8-71; (e) P12-20; (f) P12-71 with magnification 50X.

Figure 14 includes frontal views of samples P5-20-G18, P8-20-G18, and P12-20-G18, with the higher gap coating (1.500 mm) and the lower gap that provides conductivity for each one (0.750 mm for sample P5-20-G18, and 0.875 mm for P8-20-G18, and P12-20-G18), with a magnification of 50X. Blue rectangles indicate the areas of the fabric in which a valley or interstice is created by the weave pattern; yellow arrows point to uncoated or fuzzing areas.

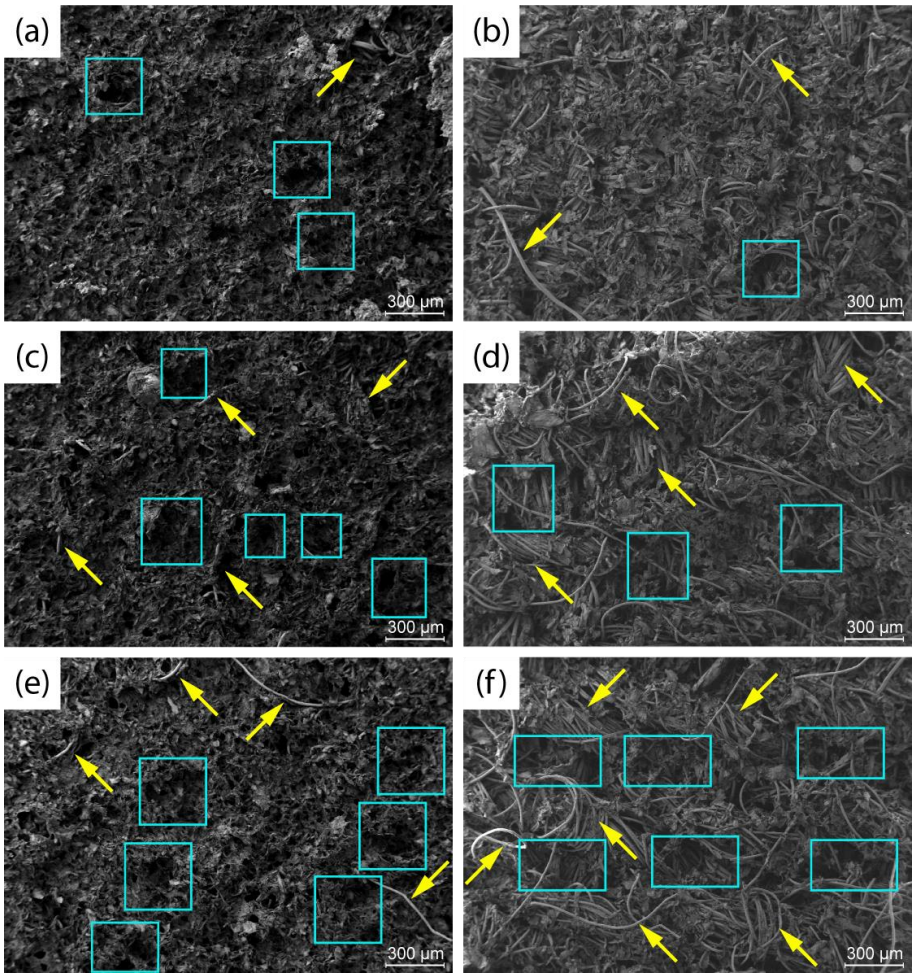

Figure 14. SEM images of samples (a) P5-20-G18$_{1.500}$; (b) P5-20-G18$_{0.750}$; (c) P8-20-G18$_{1.500}$; (d) P8-20-G18$_{0.875}$; (e) P12-20-G18$_{1.500}$; (f) P12-20-G18$_{0.875}$ with magnification 50X.

Figures 14.a and 14.b, corresponding to samples P5-20-G18$_{1.500}$ and P5-20-G18$_{0.750}$, reflect the continuity of the conductive coating obtained by satin 3e2 due to its more regular surface. Only a small area of uncoated fabric is detected, and valleys are not pronounced. On the other hand, Figures 14.c, d, e, and f showcase the unevenness of the coating because of the peaks and valleys generated by their weave patterns. The presence of fuzzy or uncoated fibers is found out both in higher and lower gaps, due to the staple nature of the yarns used to produce the fabrics. These uncoated areas will reduce the contact points between conductive particles and increase electrical resistance. Additionally, valleys are more obvious for samples P8-20 and P12-20 because of their structure. More specifically, in Figures 14.d and f, the difference between deeper and higher areas is quite noticeable, due to longer floatations in the fabric. The ample difference in height between peaks and valleys hinders contact between graphene particles, which has a significant effect on the coating conductivity, as demonstrated in Figures 5 to 7.

Figure 15 exhibits a comparison between lower conductive gap for weave patterns with weft yarn count 20 tex and weft yarn count 71.43 tex. Same color code as Figure 14 is used.

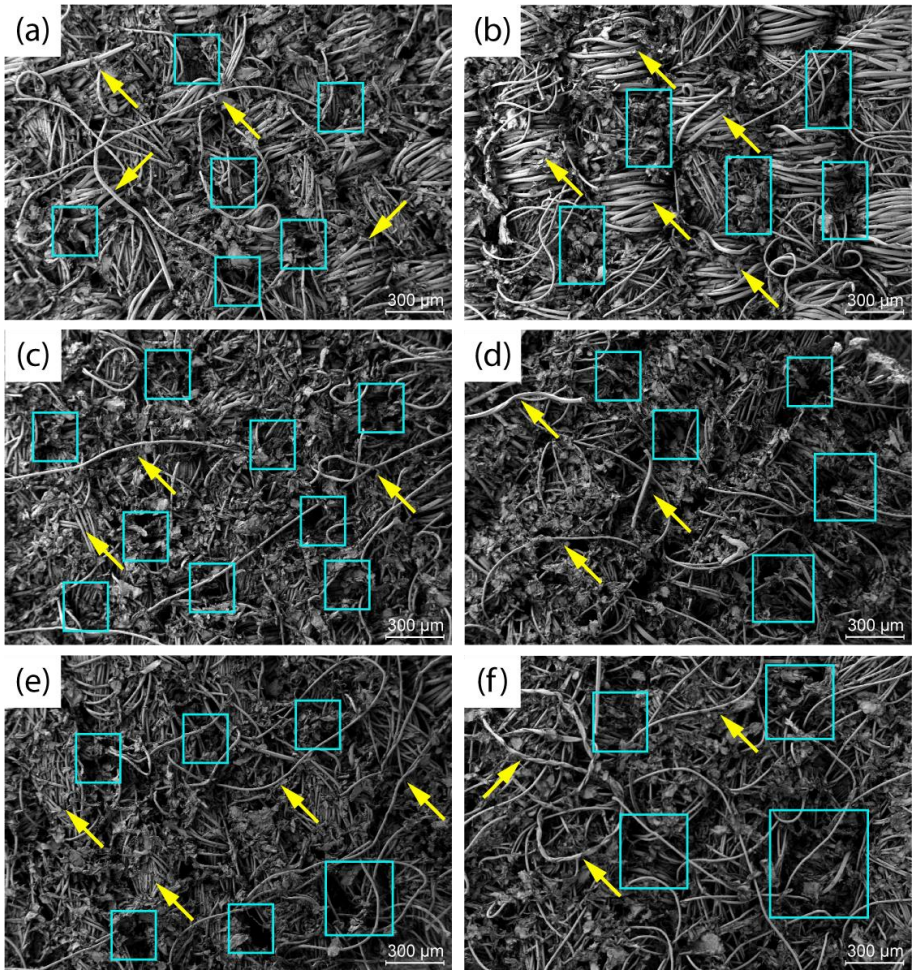

Figure 15. SEM images of samples (a) P5-20-G-24$_{0.625}$; (b) P5-71-G24$_{0.875}$; (c) P8-20-G24$_{0.750}$; (d) P8-71-G24$_{1.000}$; (e) P12-20-G24$_{0.750}$; (f) P12-71-G24$_{1.000}$ with magnification 50X.

The same trend in terms of resistance increasing when the IC decreases happens in samples with weft thread count 20 tex and 71.43 tex, which demonstrates that this effect depends on the weave pattern and its IC. In samples with thicker weft yarns, the difference in height generated between peaks and valleys is wider, so it is more difficult for graphene particles to make contact between them. Furthermore, in Figure 15.b it is clearly seen how the coating solution is deposited in the interstices and does not coat the rest of the fabric. Especially at very low gaps, the impact of thicker weft yarns on resistance values is quite noticeable, while in higher gaps, resistance values are similar in both weft thread count.

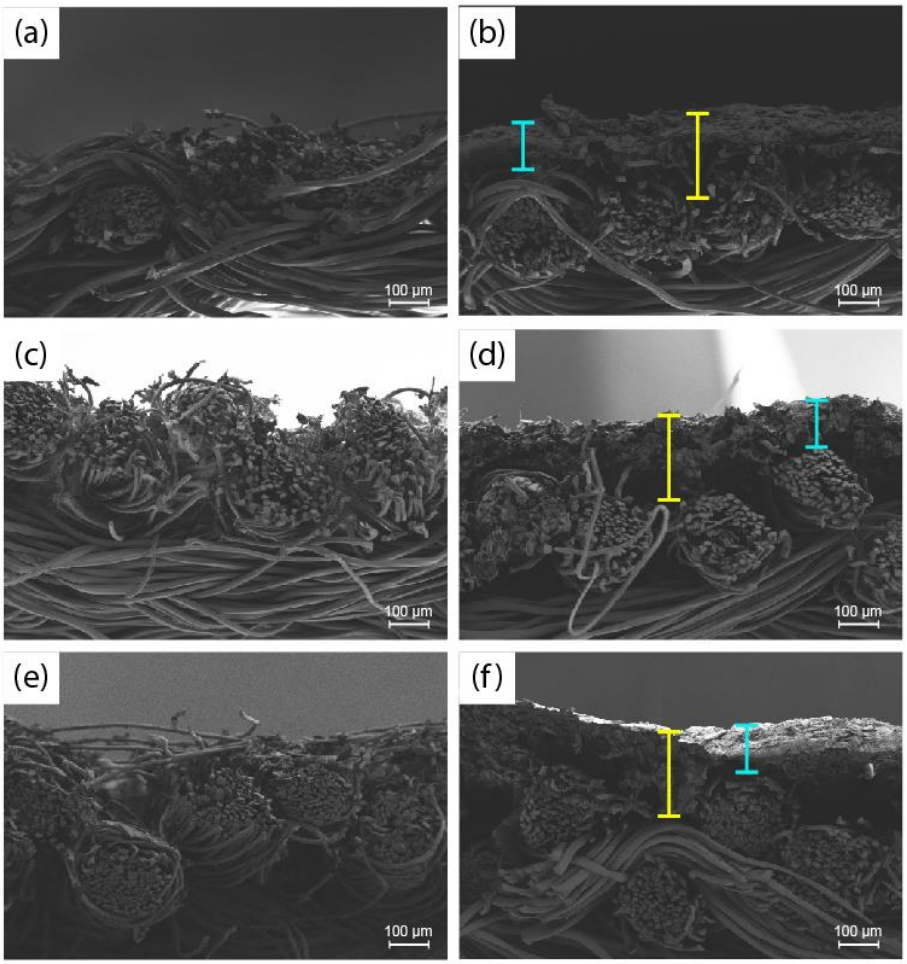

Figure 16. SEM images of samples (a) P5-20-G24$_{0.625}$; (b) P5-20-G24$_{1.500}$; (c) P8-20-G24$_{0.750}$; (d) P8-20-G24$_{1.500}$; (e) P12-20-G24$_{0.750}$; (f) P12-20-G24$_{1.500}$ with magnification 150X.

When examining the cross-sectional view of the samples in Figure 16, it is clear how the threads generate interstices where the coating is deposited. As shown in Figure 16.a, c, and e, for lower gaps the particles of graphene are practically isolated. In these images, it is observed that the coating is not homogeneous, and the graphene flakes are arranged irregularly on and between the fibers. This fact, together with the distribution of conductive particles seen in Figures 14 and 15, visually explains the high electrical resistance values obtained, since the contact between particles is interrupted by the peaks of the weave pattern. Despite this, the high specific surface of graphene,[15] makes it possible to achieve connection points between particles and produce conductivity even at lower gaps.

When the blade gap increases, the coating can bridge the fabric's peaks and generate a continuous coating, as seen in Figure 16.b, d, and f. The waviness produced by the structure of each textile can be clearly identified, with Figure 16.b having the smoothest interlacing, while Figure 16.f exhibits certain undulations, determining how the coating paste is deposited. In these images, the maximum thickness (215 µm) and the minimum thickness (120 µm) of the coating have been indicated in yellow

and blue, respectively. In the interstices of the fabric the orientation of the graphene flakes is perpendicular to the surface, while in upper areas of the coating the orientation is parallel to the fabric and the coating shows greater regularity. Some studies have proven that the relative orientations between layers of graphene determine the interaction energy between them.[39-41]

4. Conclusions

This study proves that the weave pattern and interlacing coefficient of a textile substrate significantly influence the conductivity obtained when applying a knife-coating with graphene particles. Graphene knife-coated fabrics with higher IC have better conductivity than other fabrics with the same weave pattern and lower IC. Each weave pattern generates specific interlacing points and floatations that translate to peaks and valleys, causing the coating to be deposited first in the deeper areas. It is necessary to apply coating until the height difference between peaks and valleys is bridged to achieve contact between conductive particles. This finding is of interest for coatings where the continuity of the layer is essential to ensure conductivity and useful to determine the amount of paste necessary in each case to obtain an optimal result.

Additional research to be addressed in the short term includes evaluating the influence of multiple weave patterns and different coating techniques on the conductivity results obtained. An alternative line of research with great potential is to apply this finding in textile applications where it is desired to protect a product applied to the fabric, studying how the weave pattern can facilitate the deposition of said substances in the interstices of the fabric.

To summarize, this study demonstrates that a fabric's structure influences the conductivity obtained when it is coated with graphene and serves as a starting point for further research towards this direction.

References

1. Lee C, Wei X, Kysar JW, et al. Measurement of the elastic properties and intrinsic strength of monolayer graphene. *Science* 2008.

2. Scarpa F, Adhikari S and Phani AS. Effective elastic mechanical properties of single layer graphene sheets. *Nanotechnol* 2009.

3. Huang X, Yin Z, Wu S, et al. Graphene-based materials: Synthesis, characterization, properties, and applications. *Small* 2011.

4. Castro Neto AH, Guinea F, Peres NMR, et al. The electronic properties of graphene. *Rev Mod Phys* 2009.

5. Novoselov KS, Geim AK, Morozov SV, et al. Electric field effect in atomically thin carbon films. *Science* 2004.

6. Balandin AA, Ghosh S, Bao W, et al. Superior thermal conductivity of single-layer graphene. *Nano Lett* 2008.

7. Balandin AA. Thermal properties of graphene and nanostructured carbon materials. *Nat Mater* 2011.

8. Sun Y, Wu Q and Shi G. Graphene based new energy materials. *Energy Environ Sci* 2011.

9. Brownson DAC, Kampouris DK and Banks CE. An overview of graphene in energy production and storage applications. *J Power Sources* 2011.

10. Xie J, Chen Q, Shen H, et al. Wearable Graphene Devices for Sensing. *J Electrochem Soc* 2020.

11. Depan D, Shah J and Misra RDK. Controlled release of drug from folate-decorated and graphene mediated drug delivery system: Synthesis, loading efficiency, and drug release response. *Mater Sci Eng C* 2011.

12. Matteini P, Tatini F, Cavigli L, et al. Graphene as a photothermal switch for controlled drug release. *Nanoscale* 2014.

13. Wang C, Mallela J, Garapati US, et al. A chitosan-modified graphene nanogel for noninvasive controlled drug release. *Nanomed* 2013.

14. Allen MJ, Tung VC and Kaner RB. Honeycomb carbon: a review of graphene. *Chem Rev* 2010.

15. Peigney A, Laurent C, Flahaut E, et al. Specific surface area of carbon nanotubes and bundles of carbon nanotubes. *Carbon* 2001.

16. Karim N, Afroj S, Tan S, et al. Scalable Production of Graphene-Based Wearable E-Textiles. *ACS Nano* 2017.

17. Yapici MK and Alkhidir TE. Intelligent medical garments with graphene-functionalized smart-cloth ECG sensors. *Sensors* 2017.

18. Shateri-Khalilabad M and Yazdanshenas ME. Fabricating electroconductive cotton textiles using graphene. *Carbohydr Polym* 2013.

19. Jang E, Liu H and Cho G. Characterization and exploration of polyurethane nanofiber webs coated with graphene as a strain gauge. *Text Res J* 2019.

20. Salavagione HJ, Shuttleworth PS, Fernández-Blázquez JP, et al. Scalable graphene-based nanocomposite coatings for flexible and washable conductive textiles. *Carbon* 2020.

21. Manasoglu G, Celen R, Kanik M, et al. Electrical resistivity and thermal conductivity properties of graphene-coated woven fabrics. *J Appl Polym Sci* 2019.

22. Kim H and Lee S. Characteristics of electrical heating elements coated with graphene nanocomposite on polyester fabric: effect of different graphene contents and annealing temperatures. *Fibers Polym* 2018.

23. Dong Z, Jiang C, Cheng H, et al. Facile fabrication of light, flexible and multifunctional graphene fibers. *Adv Mater* 2012.

24. Xu Z and Gao C. Graphene fiber: A new trend in carbon fibers. *Mater Today* 2015.

25. Li X, Sun P, Fan L, et al. Multifunctional graphene woven fabrics. *Sci Rep* 2012.

26. Liu X, Liu D, Lee J, et al. Spider-Web-Inspired Stretchable Graphene Woven Fabric for Highly Sensitive, Transparent, Wearable Strain Sensors. *ACS Appl Mater Interfaces* 2019.

27. Billah SMR. Textile Coatings. In: Jafar Mazumder MA, Sheardown H and Al-Ahmed A (eds) *Functional Polymers*. Cham: Springer International Publishing, 2019, p.825.

28. Hou J, Yang Y, Yu DG, et al. Multifunctional fabrics finished using electrosprayed hybrid Janus particles containing nanocatalysts. *Chem Eng J* 2021

29. Joshi M and Butola BS. 14 - Application technologies for coating, lamination and finishing of technical textiles. In: Gulrajani ML (ed) *Advances In The Dyeing And Finishing Of Technical Textiles*: Elsevier Ltd, 2013, p.355.

30. Wang L, Wang X and Lin T. Conductive coatings for textiles. In: Smith WC (ed) *Smart textile coatings and laminates*: Elsevier, 2010, p.155.

31. Wei Q, Yu L, Wu N, et al. Preparation and characterization of copper nanocomposite textiles. *J Ind Text* 2008.

32. Stankard S. Chapter 11 - Yarn to Fabric: Weaving. In: Sinclair R (ed) *Textiles and Fashion*: Elsevier Ltd, 2014, p.255.

33. Galceran V. *Weaving technology*. Terrassa: Technical University of Catalonia (in Spanish) 1962.

34. Farboodmanesh S, Chen J, Tao Z, et al. 3 - Base fabrics and their interaction in coated fabrics. In: Smith WC (ed) *Smart textile coatings and laminates*: Elsevier Ltd, 2010, p.42.

35. Backert S. The Relationship Between the Structural Geometry of a Textile Fabric and Its Physical Properties: Part II: The Mechanics of Fabric Abrasion. *Text Res J* 1951.

36. Calvimontes A, Badrul Hasan MM and Dutschk V. Effects of topographic structure on wettability of woven fabrics. *Woven Fabric Eng.Rijeka: Sciyo* 2010.

37. Özdemir H, Seçkin Uğurlu Ş and Ozkurt A. The Electromagnetic Shielding of Textured Steel Yarn Based Woven Fabrics Used for Clothing. *J Ind Text* 2015.

38. Berruezo M, Bonet-Aracil M, Montava I, et al. Preliminary study of weave pattern influence on microplastics from fabric laundering. *Text Res J* 2020.

39. Reguzzoni M, Fasolino A, Molinari E, et al. Potential energy surface for graphene on graphene: Ab initio derivation, analytical description, and microscopic interpretation. *Phys Rev B Condens Matter Mater Phys* 2012.

40. Bistritzer R and MacDonald AH. Transport between twisted graphene layers. *Phys Rev B Condens Matter Mater Phys* 2010.

41. Havener RW, Zhuang H, Brown L, et al. Angle-resolved raman imaging of interlayer rotations and interactions in twisted bilayer graphene. *Nano Lett* 2012.